*Materials and Structures*, 1995, **28**, 435–443

# Multifractal nature of concrete fracture surfaces and size effects on nominal fracture energy

ALBERTO CARPINTERI, BERNARDINO CHIAIA

*Department of Structural Engineering, Politecnico di Torino, 10129 Torino, Italy*

*Experimental evidence of the fractality of fracture surfaces has been widely recognized in the case of concrete, ceramics and other disordered materials. An investigation* post mortem *on concrete fracture surfaces of specimens broken in direct tension has been carried out, yielding non-integer (fractal) dimensions of profiles, which are then related to the 'renormalized fracture energy' of the material. No unique value for the fractal dimension can be defined: the assumption of multifractality for the damaged material microstructure produces a dimensional increment of the dissipation space with respect to the number 2, and represents the basis for the so-called multifractal scaling law. A transition from extreme Brownian disorder (slope 1/2) to extreme order (zero slope) may be evidenced in the bilogarithmic diagram: the nominal fracture energy $\mathcal{G}_F$ increases with specimen size by following a nonlinear trend. Two extreme scaling regimes can be identified, namely the fractal (disordered) regime, corresponding to the smallest sizes, and the homogeneous (ordered) regime, corresponding to the largest sizes, for which an asymptotic constant value of $\mathcal{G}_F$ is reached.*

## 1. INTRODUCTION

The remarkable observation that a characteristic feature of phase transitions is a discontinuous (catastrophic) change in the macroscopic parameters of a system undergoing continuous variation in the system state variables, leads us to set the phenomenon of fracture of disordered materials within the wide framework of critical phenomena. Moreover, the concepts of fractals (mathematical domains with non-integer dimensions) and fracture are intimately related: the word itself 'fractal' comes from the latin *fractum* which means 'broken' [1]. In the framework of critical phenomena, the universality of the behaviour at the critical point, due to the absence of a characteristic length in the process, means self-similar scaling over a broad range of scales. Self-similarity implies that a (statistically) similar morphology appears in a wide range of magnifications of the fracture surface. This means that the fractal microstructures are characterized by a low degree, and not by the absence, of order, in the sense that two subsequent points on the surface are not completely uncorrelated. The fractal dimension $D$ is then a way to quantify this 'order behind chaos', i.e., a measure of the correlation in the surface topology.

Experimental evidence of self-similarity (fractality) over a broad range of scales has been reported frequently in the recent literature: fractured surfaces of steel [2], molybdenum [3], natural rocks [4] and concrete [5], were shown to share fractal properties, at least between a scale upper bound, related to the macroscopic dimension of the object, and a scale lower bound which, depending on the material microstructure, could be set as equal to the smallest grain size or to the atomic size of its particles.

A basic question is whether any correlation exists between the fractal dimension $D$ and the physical parameters involved in the fracture process. Mandelbrot *et al.* [2] have found such a correlation between impact energy and fractal dimension, whereas other authors did not find any clear relation between $D$ and the material properties such as the fracture toughness [6].

The mechanical interpretation of the fractal dimension $D$ being greater than 2 could be that the dissipation of energy during the development of a fracture surface is something intermediate between surface energy dissipation (which is the LEFM hypothesis) and volume energy dissipation (which is the classical approach of strength of materials theories, limit analysis and damage mechanics). The definition of new mechanical 'universal' properties with (non-integer) physical dimensions depending on the fractal dimension of the damaged material microstructure represents the so-called 'renormalization' procedure, already utilized in the statistical physics of random processes [7]. In our opinion, this approach represents the right way to link fractals to mechanics, since it allows the extrapolation of the geometrical scaling properties of fractal spaces to the phenomenological scaling laws of macroscopic mechanical properties.

## 2. EXPERIMENTAL DETERMINATION OF FRACTAL DIMENSION

There are many definitions of the fractal dimension of an object, including Hausdorff dimension, Bouligand–Minkowski dimension, box-counting dimension and others. As a matter of fact, different techniques can be developed, based on such definitions, in order to extract the fractal dimension of a fracture surface or profile. Although they are all equivalent in the continuous domain and in the limit of the smallest scales, they differ

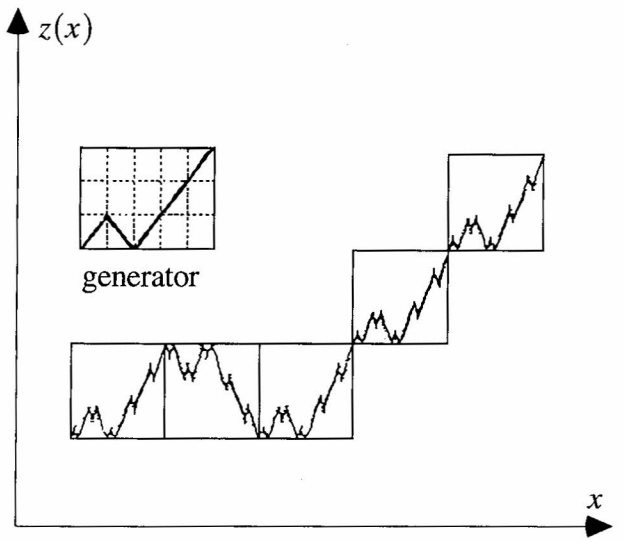


Fig. 1 Example of a (deterministic) self-affine profile.

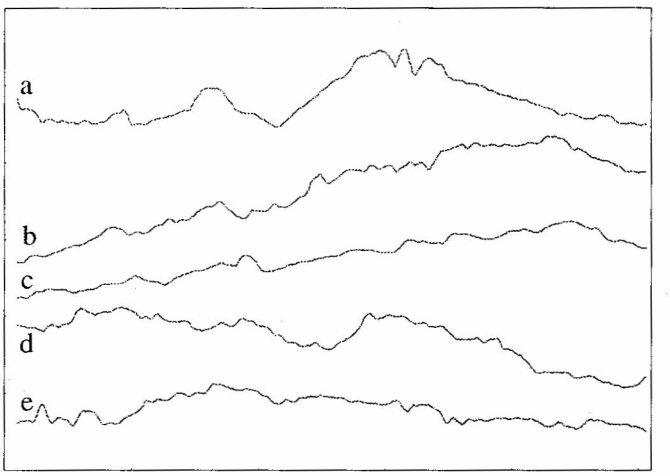


Fig. 2 Laser-digitized profiles from fracture surfaces of concrete.

substantially when discretized and applied to digitized data. Moreover, the fracture profiles of disordered materials can be better represented by 'self-affine' fractal models rather than by self-similar fractal models, and this gives rise to drawbacks in some of the techniques.

In the case of natural fractals, self-similarity means that statistically similar morphology is obtained under uniform scaling of all the coordinates. On the other hand, reliefs, landscapes and fracture surfaces reveal statistically similar morphology only if the lengths are rescaled by direction-dependent factors. Mandelbrot [8] defined this non-uniform scaling law as 'self-affinity'.

A mathematical self-affine fractal (Fig. 1) can be described by a function $z(x)$ with the following property: if the $x$ coordinate is multiplied by a scaling factor $s$, the $z$ coordinate must be scaled by a factor $s^H$:

$$z(sx) \approx s^H z(x), \quad H > 0 \tag{1}$$

where $H$ is called 'codimension'. The main feature of self-affine profiles is the presence of two different fractal dimensions, the so-called 'local' dimension and the 'global' dimension. The crossover length $t_c$ is a characteristic threshold scale of the profile, and separates two distinct regimes of scaling behaviour, depending on the length scale $L$ at which the fractal is considered: at $L < t_c$ the non-Euclidian nature of the fracture surfaces is revealed and the local non-integer dimension can be determined as $D_l = 2 - H$ (fractal or disordered regime) whereas, at $L > t_c$, the homogeneous regime, corresponding to macroscopically Euclidian behaviour, prevails. It can be demonstrated [8] that the global dimension of a self-affine profile is $D_g = 1$: therefore, if we measure the profile at scales greater than $t_c$, a dimension very close to one is obtained. This could be the reason for many anomalously low values of the fractal dimension that have been reported in the literature.

A laser profilometer has been used to scan the surfaces along several parallel profiles. A servo-controlled mechanism slowly moved the profilometer along an horizontal guide ($x$ direction) by means of a driving belt, while an automatic, computer-controlled, data acquisition system read the profile elevations ($z$ coordinate) at each step, with a vertical precision of $\pm 0.01$ mm. The profiles were discretized with a horizontal interval equal to 0.1 mm, providing 1000 points for a profile of length 10 cm. The profiles were digitized along the two main horizontal directions, in order to average out the undesired effects of an eventually present highly correlated macrocrack. Almost 70 profiles, from different specimens, have been analysed and some examples are shown in Fig. 2. Several numerical algorithms have been implemented, which are based on the definition of *compass*, *box-counting* and *spectral* dimension, in order to investigate on the fractal properties of digitized profiles.

## 3. DIVIDER METHOD

This method, also referred to as the 'yardstick' or the 'compass' method, comes from the early intuition of Richardson [9], who observed that, in the case of natural islands, the value of the coastline length obtained when measuring the perimeter by means of different gauges is not unique, and a power-law relation of coastline length versus yardstick length can be determined. Mandelbrot [1] pointed out the fundamental properties of this non-standard scaling law:

$$\log L(r) \approx (1 - D) \log r \tag{2}$$

where $L(r)$ is the length of the fractal curve measured with a yardstick of length $r$, and $D$ is the fractal dimension. The application to fracture profiles (Fig. 3a, b) consists basically of choosing subsequently smaller yardstick lengths $r_i$ and 'walking the compass' along the whole profile, measuring its total approximate length $L_i$. A limit definition holds:

$$D_c = 1 - \lim_{r_i \to 0} \frac{\log L_i}{\log r_i}, \tag{3}$$

where $D_c$ is the so-called 'compass dimension'.

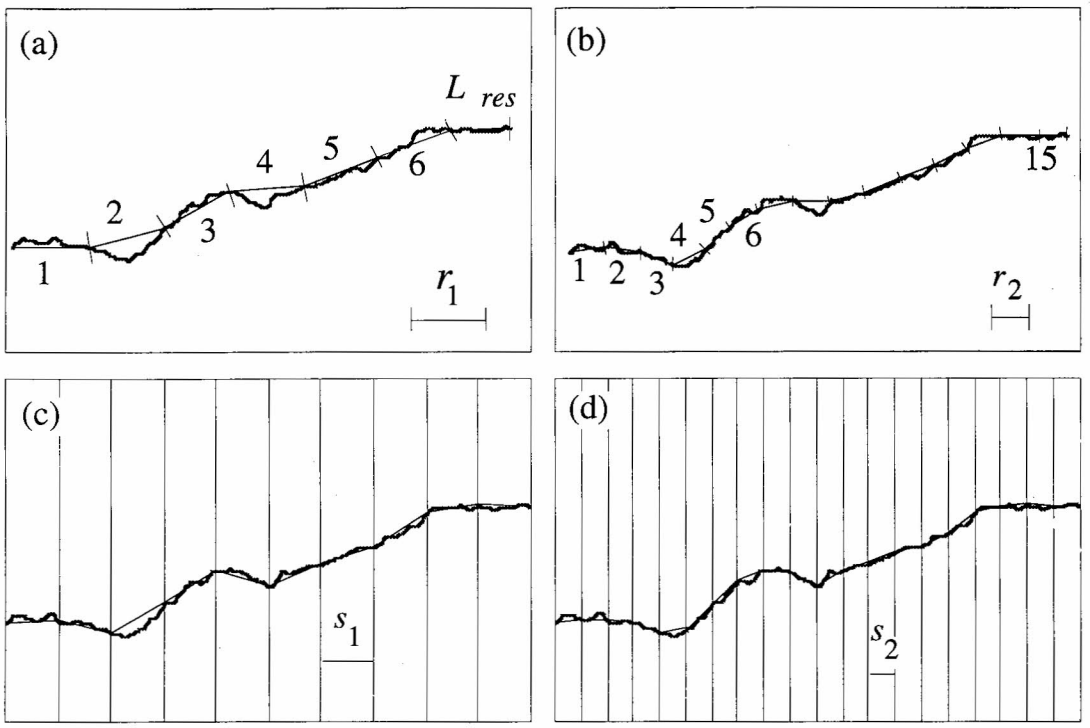


Fig. 3 Application of (a, b) the divider method and (c, d) the modified divider method to a concrete profile.

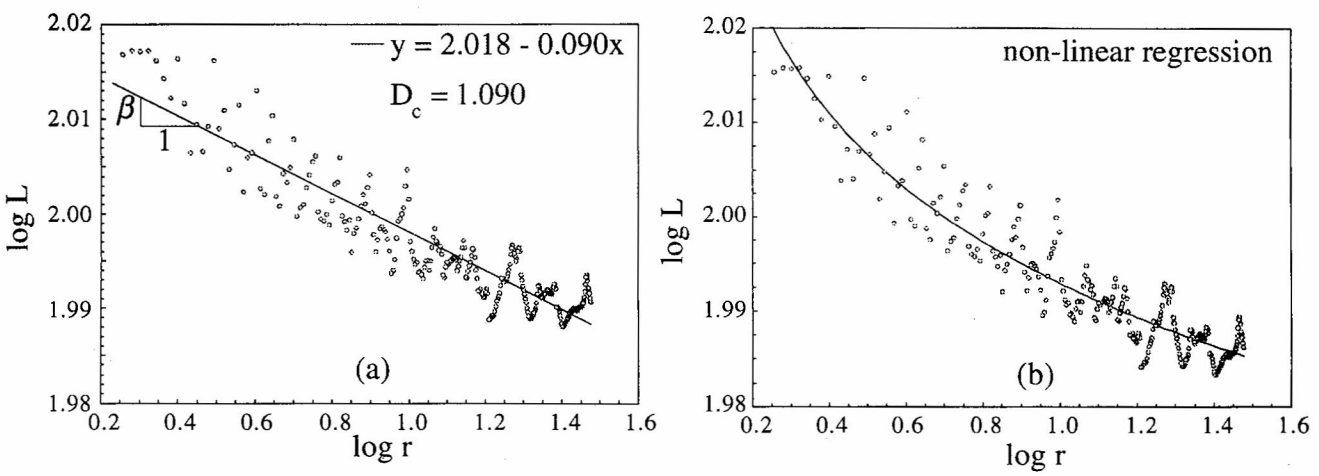


Fig. 4 Divider method: (a) monofractality versus (b) multifractality.

From an operative point of view, instead of dealing with a limit, a linear regression is performed with the bilogarithmic data ($\log L_i$ versus $\log r_i$), obtaining the slope $\beta$ (Fig. 4a). From Equation 3 it follows that $D_c = 1 + \beta$. Note that a residual length $L_{res}$ is often present at the end of the profile: it could be neglected if much smaller than the yardstick or, better, added to the approximate length or, finally, avoided, if an optimal sequence of yardsticks is used.

A modified divider method has been proposed by Brown [10]. In this case (Fig. 3c, d), the scale at which the profile length is measured is a 'projected' scale. Equally spaced intervals ($s_i$) are generated horizontally, and the approximate length of the profile is computed by summing the distances between two subsequent intersections on the profile. A dyadic sequence with subsequently smaller intervals is preferable in order to avoid residual lengths: $s_1$, $s_1/2$, $s_1/4$, $s_1/8$ and so on. A drawback when using a dyadic sequence is that the divider rapidly reaches the digitization precision: only a few points can then be plotted in the bilogarithmic diagram, so that a best fit could be elusive.

The compass dimension, which coincides exactly with the Hausdorff dimension in the case of self-similar fractals, cannot be defined unequivocally in the case of self-affine profiles. The yardstick of length $r_i$, walked along the curve, scales in a homogeneous manner in both the $x$ and $y$ directions, whereas non-uniform (direction dependent) scaling is required by self-affinity. It can be

shown [11] that the compass dimension is $D_c = 1/H$ in the limit where the $z$ scale is magnified, i.e., when we multiply the profile heights by 100 or 1000, whereas a global dimension equal to the topological one ($D_g = 1$) is obtained if the fluctuations $z(x)$ are smoothed, that is, for large scales of observation. Thus, assuming that a local limiting value $1/H$ is reached by the compass dimension $D_c$ when the profile heights are properly magnified, the fractal dimension ($D = 2 - H$) of a self-affine profile could be computed as $D = 2 - 1/D_c$. The local limit $1/H$ of the compass dimension for self-affine profiles is sometimes called the 'latent' fractal dimension [1].

In Fig. 4 the application of the method to a concrete profile is presented. When the yardstick's length becomes comparable with the digitization interval (i.e., 0.1 mm), discreteness effects come into play, no fractality can be revealed and, therefore, the related points are neglected. With reference to Fig. 4a (the so-called Richardson's plot), linear regression provides $D_c = 1 + \beta = 1.09$, which turns out to be too low. It can be argued that this is due to the self-affine scaling behaviour. Performing the compass analysis on the transformed profile ($z^* = z \times 100$), yields $D_c = 1.21$, which is a more consistent value. On the other hand, Fig. 4b shows a nonlinear fit of $L_i$ versus yardstick length and, more precisely, a continuously decreasing fractal dimension with increasing scale length, which is clearly a more realistic interpretation of the fractal behaviour of fracture surfaces. Note that, from a mathematical point of view, the upward concavity in the log $L_i$ versus log $r_i$ plot is the major clue to fractality, since it implies non-differentiability of the profile [11]. The asymptotic limit for the largest scales is $D_c = 1$, which corresponds to macroscopic homogeneity and to the global dimension of self-affinity theory. Regarding the small scale behaviour (fractal or disordered regime), a limiting local value of $D_c = 1.39$ has been revealed by our analysis. A deeper resolution of the data digitization is required, nevertheless, in order to investigate on the fractal regime at the smallest scales. It could be shown finally that the modified dividers method yields practically the same results through the whole range of scales.

## 4. BOX-COUNTING METHOD

This method comes from the original definition of covering dimension due to Bouligand [12], with the difference that, instead of a 'sausage' defined as the union of all the disks with radius $\varepsilon$ centred on the profile (that is, the set of all the points within a distance $\varepsilon$ from the profile), a 'generalized cover' with square grids is used. If $E$ is the fractal profile, $N(E, \varepsilon)$ is defined as the smallest number of boxes with linear size $\varepsilon$ needed to cover $E$. If the limit:

$$\lim_{\varepsilon \to 0} \frac{\log N(E, \varepsilon)}{\log (1/\varepsilon)} = D_b, \tag{4}$$

exists and is finite, then $D_b$ is called the box-counting dimension of $E$. In analogy with the Minkowski–Bouligand definition of covering dimension, if $|\mathbf{E}(\varepsilon)|_2$ is the area of this generalized cover ($|E(\varepsilon)|_2 = N(E, \varepsilon)\,\varepsilon^2$), the following relation also holds:

$$D_b = 2 - \lim_{\varepsilon \to 0} \frac{\log |E(\varepsilon)|_2}{\log \varepsilon}. \tag{5}$$

From an operative point of view, the box-counting method is implemented by generating a square grid of linear dimension $\varepsilon_i$ and determining the number $N_i(E, \varepsilon_i)$ of boxes needed to cover the entire profile or, equivalently, their total area $|E(\varepsilon)|_2$ (Fig. 5a,b). The procedure is repeated with progressively smaller box sizes. Linear regression with the bilogarithmic data (log $N_i$ versus log $\varepsilon_i$) is performed, and the fractal dimension is obtained from the slope $\alpha$ of the best-fitting line: from Equation 4 it follows that $D_b = \alpha$. The best results are obtained by computing $N_i$ with different origins of the grid, and then averaging out, in order to extract a more objective value.

The application of the method to a concrete profile is presented in Fig. 6, where the main discreteness effects have been eliminated previously. A fractal dimension of

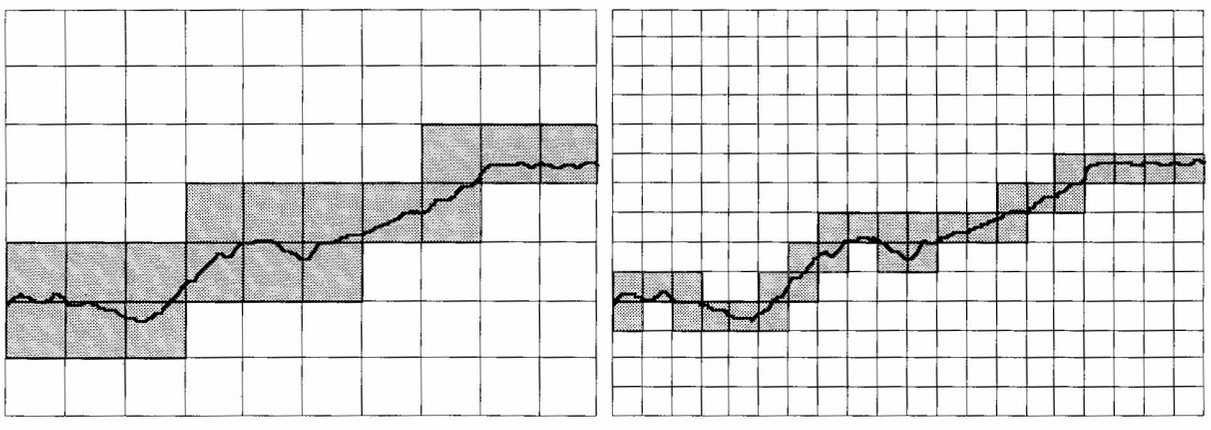

(a) (b)

Fig. 5 Application of the box-counting method to a concrete profile.

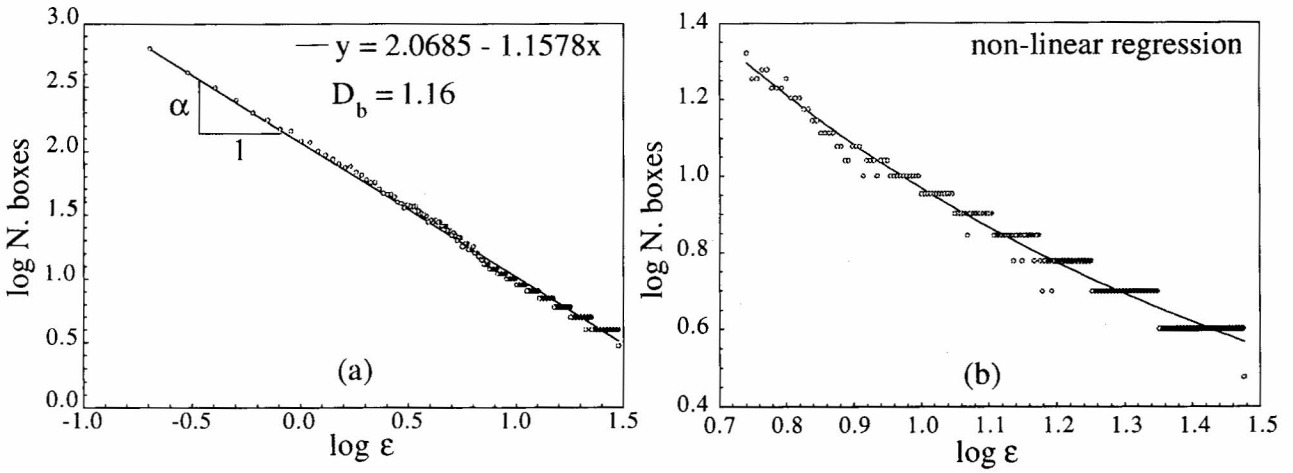


Fig. 6 Box-counting method: (a) monofractality versus (b) multifractality.

1.16 is provided by linear regression of the logarithmic data (Fig. 6a) whereas, for the same profile, the compass method yielded 1.09. A nonlinear fit of the same data is shown in Fig. 6b, yielding a more reliable interpretation of the fractal behaviour: $D_b$ decreases continuously with increasing box size. All the profiles examined showed the same behaviour, which can thus be considered as a universal property of these multifractal sets. Note the stability of the method with respect to the divider method: although the crossover length problem is still present, far fewer oscillations are revealed at the largest scales.

On the other hand, a measure of the Bouligand type is not well adapted to a self-affine set. In fact, the direction-dependent scaling of self-affine profiles provides an inconsistency when the covering is made by homothetically decreasing square boxes. An affine scaling of the boxes (that is, if $b$ is the scaling ratio in the $x$ direction, $b^H$ is the ratio in the $z$ direction) should be performed, and an iterative procedure should be used since the exponent $H$ is unknown. In order to obtain magnification of profile heights, rectangular boxes can be used with the vertical side much lower than the horizontal, so that the local fractal dimension ($D = 2 - H$) can be extracted. Profile height magnification may also be obtained by simply multiplying the vertical coordinates by, for example, 100, and covering the profile by the usual self-similar square mesh. Anyway, the local fractal value is reached only in the higher resolution of the covering process, whereas, as in the case of square boxes, we will always measure the global dimension ($D_g = 1$) if we keep increasing the box size.

## 5. STATISTICAL APPROACH: THE SPECTRAL METHOD

The methods illustrated previously are all derived from a deterministic approach. The spectral method, on the other hand, comes from statistical arguments. The profile is considered as a randomly varying quantity in space, and its fractal dimension is obtained by a stochastic analysis of this behaviour. This last method may be proved rigorously only for self-affine profiles, since the fundamental relations between the statistical quantities and the fractal dimension can be obtained only on the basis of the self-affinity hypothesis [13]. The classical statistical quantities, in the case of discretized profiles, are the mean and the variance of surface elevations, respectively $\mu = (1/n)\sum z_i$ and $\sigma^2 = (1/n)\sum (z_i - \mu)^2$, where $n$ is the number of digitized points and $z_i$ are their elevations. Since the simple statistical parameters do not provide any information about the correlation among the profile elevations, no relation with the fractal dimension can be obtained from $\mu$ and $\sigma^2$. However, a Fourier decomposition of the profiles (considered as noises in the space) can be performed in order to extract the degree of correlation of the fracture locus over the whole spatial frequency spectrum.

It has been demonstated [13] that, for noises in time, the power spectrum $S$ versus frequency $f$ shows power-law behaviour: $S(f) \approx f^{-\beta}$, where the exponent $\beta$ inceases with increasing correlation in the noise, i.e., with decreasing randomness. The white noise is the most random, in the sense that it is completely uncorrelated: the position of a point is completely independent of that of the other points. Its power spectrum shows a constant intensity at all frequencies (like a white light) and therefore $\beta = 0$. The fractal dimension of white noise can be determined easily as $D = 2$ [11].

The fracture surface can be considered as a randomly varying quantity $z(x, y)$ in space. Unlike white noise, the phenomenon of fracture is neither completely random nor completely correlated: therefore fractional Brownian motions [14] are better suited to model fracture profiles. The local breaking rule obviously depends on the (randomly distributed) material properties, but also on the surrounding stress–strain state, which becomes increasingly important as the external load increases (i.e., when the critical load is approached). Post-critical behaviour, in particular, corresponds to a highly correlated development of the fracture surface.

The application of the spectral method to fracture profiles, in order to extract their fractal dimension,

basically consists of performing the discrete fast Fourier transform of the vector $Z$ of equally spaced profile heights, in order to obtain the vector $F = \mathrm{FFT}(Z)$ of complex coefficients in the frequency domain. This implies the decomposition of the profile trace into the sum of many sine and cosine terms, each with its own amplitude and frequency. Then the power spectral density $S(f)$ is determined, where $S(f)\,\mathrm{d}f$ is the contribution to the total power from components in the profile with frequencies between $f$ and $f + \mathrm{d}f$:

$$S(f) = \frac{1}{L} F \,\mathrm{conj}(F) \tag{6}$$

where $L$ is the horizontal projection of the profile. The bilogarithmic data $\log S(f)$ versus $\log f$ are plotted and then fitted by linear regression. From the slope $\beta$ of the best-fitting line, the fractal dimension can be obtained as:

$$D_s = \frac{5 - \beta}{2} \tag{7}$$

The above relation between the 'spectral' dimension $D_s$ and the spectral slope $\beta$ could be demonstrated, based on the self-affinity hypothesis, by means of the '2-point autocorrelation function' [13].

It is worth pointing out that, generally, this method provides overestimation of fractal dimensions lower than 1.5, while an underestimation results if the dimension is greater than 1.5. In any case, for the relationship between spectral slope and fractal dimension to yield reliable results [15], the slope must lie in the range $2 \leq \beta \leq 3$, giving fractal dimensions between 1 and 1.5. If $\beta > 3$ we have to consider $D_s = 1$, the profile being differentiable (in other words, it is not a fractal), whereas, if $\beta < 2$, overhangs may be present in the profile, which are missed by the spectral analysis. On the other hand, since stationarity is a fundamental assumption in Fourier theory, the profile traces have to be detrended before taking the transform, otherwise an anomalous overestimation of $D$ is obtained [15]. The detrending of the profile is obtained simply by minimizing the variance of surface elevations (Fig. 7). Beyond these slight drawbacks, the main advantage of the stochastic approach is that the crossover length problem becomes obviously much less important than in the case of deterministic methods.

An application of the spectral method to a digitized profile is shown in Fig. 8, where the logarithmic data $\log S(f)$ versus $\log f$ have been correlated by linear regression (Fig. 8a) and nonlinear fitting (Fig. 8b),

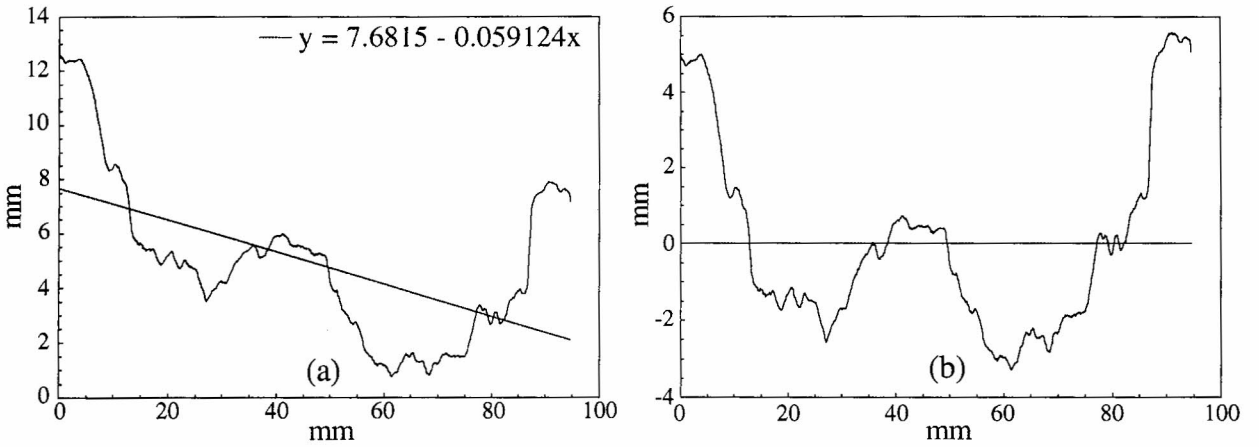


Fig. 7 Digitized concrete profile (a) prior and (b) after detrending.

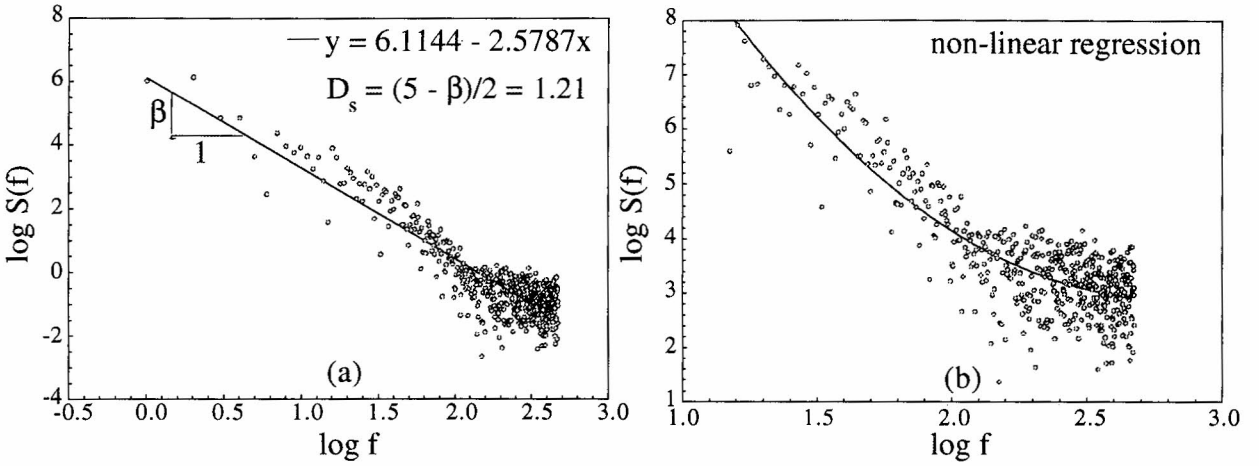


Fig. 8 Spectral method: (a) monofractality versus (b) multifractality.

respectively. The fractal analysis was performed on a detrended profile, yielding, in the case of linear fitting, a slope $\beta = 2.58$. From Equation 7, the corresponding fractal dimension is $D_s = 1.21$. Note that the same profile, prior to detrending, gave $D_s = 1.48$, which therefore results in an inconsistent value.

Nonlinear regression (Fig. 8b) confirms the multifractal nature previously recognized by means of the deterministic methods. In fact, a continuously decreasing spectral slope $\beta$ with increasing frequency can be evidenced, thus implying a continuously decreasing fractal dimension $D_s$ with increasing wavelength $\lambda$, i.e., with increasing scale length ($\lambda = 1/f$).

## 6. SIZE EFFECT ON NOMINAL FRACTURE ENERGY: AN EXPLANATION BASED ON A (MONOFRACTAL) RENORMALIZATION GROUP PROCEDURE

We can detect an evident mechanical consequence of the fractality of fracture surfaces, considering the size effects on fracture energy $\mathcal{G}_F$. Since Hillerborg's proposal for a concrete fracture test was published as a RILEM Recommendation [16], several researchers have measured a fracture energy $\mathcal{G}_F$ which increases with specimen size and, more specifically, with the size of the uncracked ligament. Such a trend has been systematically found, and in each case the authors of the papers describing these experiments have tried to provide various empirical or phenomenological explanations, without, however, endeavouring to interpret their findings in a larger conceptual framework.

The assumption of a monofractal surface of dissipation implies geometrical self-similar scaling. On the other hand, scale-invariance forms the basis of renormalization group theory, which has been applied successfully to the analysis of continuous phase-transitions, and has provided a basis for calculations of the universal critical exponents, which are confirmed to be non-integer numbers.

Based on the hypothesis of scale-invariance and supposing, for the fracture surface, a fractal dimension $D = 2 + d_{\mathcal{G}}$, a way of explaining the increase in the fracture energy with specimen size is that of considering a sequence of scales of observation [17]. Since the total energy $W$ dissipated by fracture is a macroscopic quantity, thus invariant with respect to the scale of observation, we have:

$$W = \mathcal{G}_1 A_1 = \mathcal{G}_2 A_2 = \cdots = \mathcal{G}_{n-1} A_{n-1} = \mathcal{G}_n A_n = \mathcal{G}_{n+1} A_{n+1} = \cdots = \mathcal{G}_\infty A_\infty \quad (8)$$

where the first scale of observation could be the macroscopic one, with $\mathcal{G}_1 A_1 = \mathcal{G}_F A$, $A$ and $\mathcal{G}_F$ being respectively the nominal cross-sectional area and the RILEM fracture energy [16], and the asymptotic scale of observation could be the microscopic one, with $\mathcal{G}_\infty A_\infty = \mathcal{G}_F^* A^*$, $A^*$ being the 'measure' ($[L]^{2+d_{\mathcal{G}}}$) of the fractal set representing the irregular fracture surface and

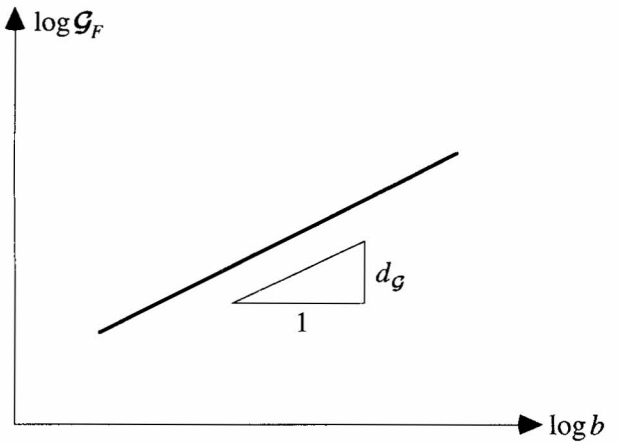


Fig. 9 Size effect on nominal fracture energy (monofractality).

$\mathcal{G}_F^*$ the 'renormalized fracture energy' with dimensions $[F][L]^{-(1+d_{\mathcal{G}})}$. From the equality between the extreme members of Equation 8, we obtain

$$\mathcal{G}_F = \mathcal{G}_F^*\left(\frac{A^*}{A}\right) \approx \mathcal{G}_F^*\left(\frac{b^{2+d_{\mathcal{G}}}}{b^2}\right) \quad (9)$$

where $b$ is the characteristic dimension of the cross-section. From Equation 9:

$$\log \mathcal{G}_F = \log \mathcal{G}_F^* + d_{\mathcal{G}} \log b \quad (10)$$

which implies a linear variation in the bilogarithmic diagram (Fig. 9).

When $d_{\mathcal{G}} = 0$, we find again the classical RILEM fracture energy, and no size effect can be detected. When $d_{\mathcal{G}} = 1$, as a limit case, $\mathcal{G}_F^*$ assumes the dimensions of energy per unit volume, as is usually the case for the plasticity or damage mechanics critical energy. Nevertheless, the latter value represents only a theoretical abstraction, since the physical limit for $d_{\mathcal{G}}$ seems to be equal to 0.5, as will be explained next.

Renormalization group relations analogous to Equation 10 have been proposed by Wilson [7] in statistical physics, as well as by Barenblatt [18] in the intermediate asymptotics description of turbulence and blasting.

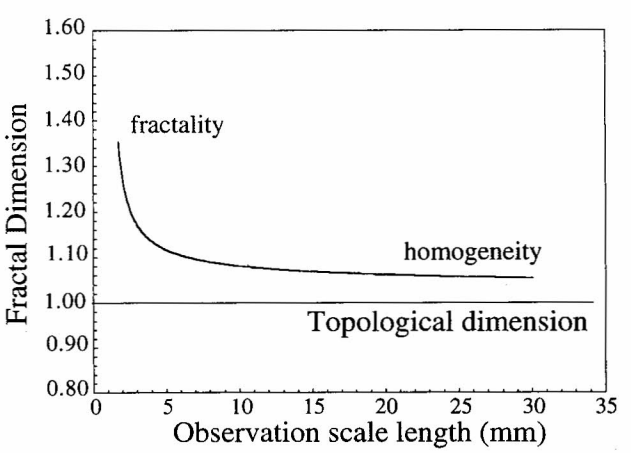


Fig. 10 Geometrical multifractality: progressive smoothing of disorder with increasing observation scale length.

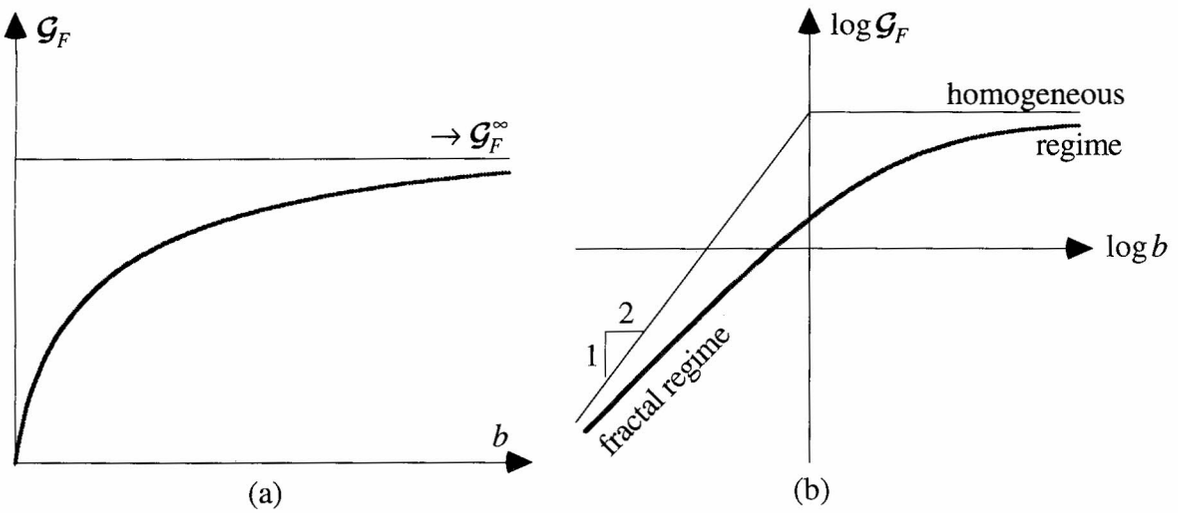


Fig. 11 Multifractal scaling law for fracture energy: (a) proportional versus (b) bilogarithmic diagrams.

## 7. MULTIFRACTAL SCALING LAW FOR THE NOMINAL FRACTURE ENERGY: TRANSITION FROM A BROWNIAN DISORDER TO AN ASYMPTOTIC ORDER

Self-affinity theory states that two dimensions can be determined for each profile: the (non-integer) local dimension, in the limit of scales tending to zero, and the global dimension, corresponding to the largest scales, which is equal to 1 (or, equivalently, for a fractal surface, equal to 2). Regarding the scaling behaviour of surfaces, our experimental results have confirmed the asymptotic smoothing of fractality (homogeneous regime) for increasing scale lengths but, generally, it appears more consistent to deal with a continuous variation of the fractal dimension against the scale length (geometrical multifractality) than to consider only two limit values of the fractal dimension (Fig. 10).

A strong physical correspondence with the geometrical trend can be emphasized: 'the effect of microstructural disorder on mechanical behaviour becomes progressively less important at larger scales, whereas it represents the fundamental feature at smaller scales'. Thus, if we consider a continuously decreasing fractal increment $d_{\mathcal{G}}$ with increasing scale of observation, Equation 10 ceases to be representative and a nonlinear trend (multifractal scaling law) emerges, according to the progressive smoothing and eventual disappearance of disorder with increasing scale ($A_{n+1}/A_n \rightarrow 1$ for $b \rightarrow \infty$). It can thus be said that, for large structures (i.e., large when compared with the microstructural characteristic size), the disordered (damaged) microstructure is somehow homogenized, that is, it behaves macroscopically as an ordered microstructure (homogeneous regime).

According to the multifractal scaling law (Fig. 11a,b), the scale effect should vanish in the limit of structural size $b$ tending to infinite, where an asymptotic value of $\mathcal{G}_F$ can be determined. On the other hand, for small specimens, the effect of the disordered microstructure becomes progressively more important, and $\mathcal{G}_F$ decreases with decreasing size, ideally tending to zero. In the bilogarithmic diagram the slope locally represents the fractal dimensional increment $d_{\mathcal{G}}$ which can be assumed as a measure of the variable influence of disorder on the mechanical behaviour. Two limit conditions have to be satisfied: $d_{\mathcal{G}} \rightarrow 0$ for large structures, and $d_{\mathcal{G}} \rightarrow 0.5$ for small structures. The last situation corresponds to the highest possible disorder, the 'Brownian' disorder, which is a theoretical upper bound.

The dimensional bound $d_{\mathcal{G}} \leq 0.5$ has been pointed out already by Carpinteri [19] using dimensional analysis arguments, and relating the dimensional increment $d_{\mathcal{G}}$ of the fracture surface to the dimensional decrement $d_\sigma$ of the tensile ligament at the critical point. The latter, in its turn, is responsible for the scaling behaviour of nominal tensile strength [20], and is found to be equally bounded: $d_\sigma \leq 0.5$.

## ACKNOWLEDGEMENTS

The present research was carried out with the financial support of the Ministry of University and Scientific Research (MURST) and the National Research Council (CNR).

## REFERENCES

1. Mandelbrot, B. B., 'The Fractal Geometry of Nature' (W. H. Freeman, New York, 1982).
2. Mandelbrot, B. B., Passoja, D. E. and Paullay, A. J., 'Fractal character of fracture surfaces of metals', *Nature* **308** (1984) 721–722.
3. Sumiyoshi, H., Matsuoka, S., Ishikawa, K. and Nihei, M., 'Fractal characteristics of scanning tunneling microscopic images of brittle fracture surfaces on molybdenum', *Soc. mech. Engrs Int. J.* **35** (1992) 449–455.
4. Brown, S. R. and Scholz, C. H., 'Broad bandwidth study of the topography of natural rock surfaces', *J. geophys. Res.* **90** (1985) 12575–12582.

5. Saouma, V. E., Barton, C. C. and Gamaleldin, N. A., 'Fractal characterization of fracture surfaces in concrete', *Engng Fracture Mech.* **35** (1990) 47–53.
6. Davidson, D. L., 'Fracture surface roughness as a gauge of fracture toughness: aluminium-particulate SiC composites', *J. Mater. Sci.* **24** (1989) 681–687.
7. Wilson, K. G., 'Renormalization group and critical phenomena', *Phys. Rev.* **B4** (1971) 3174–3205.
8. Mandelbrot, B. B., 'Self-affine fractals and fractal dimension', *Physica Scripta* **32** (1985) 257–260.
9. Richardson, L. F., 'The problem of contiguity: an appendix of statistics of deadly quarrels', *General System Yearbook* **6** (1961) 139–187.
10. Brown, S. R., 'A note on the description of surface roughness using fractal dimension', *Geophys. Res. Lett.* **14** (1987) 1095–1098.
11. Feder, J., 'Fractals' (Plenum Press, New York, 1988).
12. Bouligand, G., 'Sur la notion d'ordre de mesure d'un ensemble plan', *Bull. Sci. Math*, **II-52** (1929) 185–192.
13. Voss, R. F., 'Random fractal forgeries', in 'Fundamental Algorithms for Computer Graphics', edited by R. A. Earnshaw (Springer-Verlag, Berlin, 1985) 805–835.
14. Mandelbrot, B. B. and Van Ness, J. W., 'Fractional Brownian motions, fractional noises and applications', *SIAM Rev.* **10** (1968) 422–437.
15. Hough, S. E., 'On the use of spectral methods for the determination of fractal dimension', *Geophys. Res. Lett.* **16** (1989) 673–676.
16. RILEM Technical Committee 50, 'Determination of the fracture energy of mortar and concrete by means of three-point bend tests on notched beams', Draft Recommendation, *Mater. Struct.* **18** (1985) 287–290.
17. Carpinteri, A. and Chiaia, B., 'Fractals, renormalization group theory and scaling laws for strength and toughness of disordered materials', in 'Proceedings of the Workshop Probabilities and Materials: Tests, Models and Applications (PROBAMAT)', Cachan, France, November 1993 (Kluwer, Dordrecht, 1994) pp. 141–150.
18. Barenblatt, G. I., 'Similarity, Self-Similarity and Intermediate Asymptotics' (Consultant Bureau, New York, 1979).
19. Carpinteri, A., 'Scaling laws and renormalization groups for strength and toughness of disordered materials', *Int. J. Solids Struct.* **31** (1994) 291–302.
20. Carpinteri, A., Chiaia, B. and Ferro, G., 'Multifractal nature of material microstructure and size effects on nominal tensile strength', in 'Proceedings of the IUTAM Symposium on Fracture of Brittle Disordered Materials: Concrete, Rock and Ceramics', Brisbane, Australia, September 1993 (E & FN Spon, London, 1994) pp. 21–34.

## RESUME

**Nature multifractale des surfaces de rupture du béton et effets d'échelle sur l'énergie de rupture**

*On a largement établi la preuve expérimentale du caractère fractal des surfaces de rupture dans le cas du béton, des céramiques et d'autres matériaux 'désordonnés'. Une étude* post mortem *menée sur des surfaces de rupture d'échantillons cassés par traction directe révèle des dimensions non intégrales (fractales) des profils dont on a établi la relation avec l'énergie de rupture 'renormalisée' du matériau. Il n'est pas possible d'établir une valeur unique de la dimension fractale: en présumant la multifractalité de la microstructure du matériau endommagé, on obtient une augmentation dimensionnelle par rapport au numéro 2 et on établit la base de la loi dite d'échelle multifractale. Dans le diagramme à deux logarithmes on peut voir une transition du désordre de Brown extrême (inclinaison 1/2) à l'ordre extrême (inclinaison zéro); l'énergie de fracture nominale $\mathcal{G}_F$ augmente avec les dimensions de l'échantillon suivant une tendance non linéaire. On peut voir deux régimes extrêmes d'échelle, c'est-à-dire le régime fractal désordonné), qui correspond aux dimensions minimales, et le régime homogène (ordonné), qui correspond aux dimensions maximales pour lesquelles on atteint une valeur constante asymptotique de $\mathcal{G}_F$.*